

## Quasi-stationary phase change heat transfer on a fin

Tadeusz Orzechowski<sup>1,a</sup>, Katarzyna Stokowiec<sup>1</sup>

<sup>1</sup>Kielce University of Technology, 25-314 Kielce, Al. 1000-lecia P.P. 7, Poland

**Abstract.** The paper presents heat transfer research basing on a long fin with a circular cross-section. Its basis is welded to the pipe where the hot liquid paraffin, having a temperature of 70°C at the inflow, is pumped. The analyzed element is a recurrent part of a refrigeration's condenser, which is immersed in a paraffin. The temperature of the inflowing liquid is higher than the temperature of the melting process for paraffin, which allows the paraffin to liquify. The temperature at the basis of the rib changes and it is assumed that the heat transfer is quasi-stationary. On this basis the estimation of the mean value of heat transfer coefficient was conducted. The unsteady thermal field of the investigated system was registered with an infrared camera V50 produced by a Polish company Vigo System. This device is equipped with a microbolometric detector with  $384 \times 288$  elements and the single pixel size  $25 \times 25 \mu\text{m}$ . Their thermal resolution is lower than 70 mK at a temperature of 30 °C. The camera operates at  $7,5 \div 14 \mu\text{m}$  long-wave infrared radiation range. For a typical lens 35 mm the special resolution is 0.7 mrad. The result of the calculations is mean heat transfer coefficient for the considered time series. It is equal to  $50 \text{ W m}^{-2} \text{ K}^{-1}$  and  $47 \text{ W m}^{-2} \text{ K}^{-1}$  on the left and right side of the fin, respectively. The distance between the experimental data and the curve approximating the temperature distribution was assessed with the standard deviation,  $S_d = 0.04 \text{ K}$ .

### 1 Introduction

There are multiple energy saving requirements both in residential and industrial constructions. They include statutory restrictions dealing with low heat transfer coefficients in each of the building partitions on one hand and an increased necessity of heat recovery applications and absorption of mostly renewable energy on the other. Currently employed methods with sensible heat storage are not effective enough due to the possible short time of its storage. Therefore phase change materials (PCM) can be a promising alternative used in order to absorb latent energy. They seem to be a solution to the problems of sensible systems since they work during phase change process and thus stabilize the temperature [1]. Latent heat is usually produced through solidification or melting.

The multiple advantages of energy storage with phase change materials predispose this kind of installation as preferable applications. Phase change process can be applied in many areas where solar energy absorption systems with solar collectors are used [2]. The application of phase change materials allows to acquire the proper microclimate conditions inside rooms while energy is stored for heating [3] and domestic hot water [4] purposes. On the other hand cool absorption by means of PCM is also possible for air-conditioning or free-cooling purposes [5]. The processes mentioned can be

delivered by filling the proper tank with PCM and storage of energy gained for long periods of time [6]. The other possibility is to build the phase change material in the building structure. It allows to decrease the influence of temperature change inside the room on microclimate [7]. Such an installation may also absorb heavy heat fluxes that may be derived from fire flames [8] and constitute the passive element of fire-fighting protection. Phase change processes can be also applied in inactive road defrost [9] decreasing the exploitation costs and eliminating the dependence on mobility of traffic maintenance workers. This kind of solution brings advantages both in economic and ecologic aspects not only to the direct user.

In order to select the PCM suitable for the required system it is necessary to learn the thermal features of the substance chosen such as heat capacity, phase change heat and melting temperature [10]. Phase change materials are diverse. There are organic substances such as fatty acids, esters or paraffin and non-organic ones such as salts or hydrated salts among the PCMs [11]. When taking into consideration the last-mentioned ones we observe the disadvantages of supercooling and phase separation during heat absorption. The issues can be limited with sodium chloride solution addition [12]. As for the organic substances the low thermal conductivity problem is the drawback and can be solved by

<sup>a</sup>Corresponding author: todek@tu.kielce.pl

encapsulation [13] as well as application of multiple nanoparticles additives such as boron nitrate [14] or cement composites [15]. The research presents other study areas. Shell materials are employed in order to create capsules. It contributes to the limitation of natural convection processes during the phase change in favor of enhancing the thermal conductivity [16]. The combination of paraffin with nanoparticles of iron oxide  $\text{Fe}_3\text{O}_4$  seems to be a very promising method since it results in an increase of thermal conductivity by ca. 8 % [17]. The shape of the tank as well as the distance between PCM and the tank's wall are also significant factors since they affect the dynamics of the process [18].

The correct selection of phase change material for the process required involves the analysis of some parameters of the material chosen. First of all, it is necessary to learn the latent heat of fusion and the melting temperature. Therefore the paraffin can be applied in cooling installations as well as in order to satisfy the users' needs for domestic hot water [19].

Accumulation of heat that can be used for future purposes requires the installation of different kinds of tanks. The most effective ones employ the phase change processes. The loading of the PCM tank is conducted when the energy is available while the discharging process proceeds during the peak heat or cool demand hours. Both processes take place in a relatively short period of time. That is why the heat exchanger needs to be designed with a highly developed surface that is usually finned. In order to improve the heat transfer some surface modifications can also be applied [20, 21]. Experimental results are used in case of calculation procedures for heat exchangers working during the phase change process [22].

It is required to learn the heat transfer coefficient in order to design and optimize the construction of such installations. Unfortunately the availability of these data for phase change systems is insufficient. Therefore the aim of this paper is the study of methodology and measurement of heat transfer coefficient for a finned heat exchanger with paraffin filling.

## 2 Methodology

Heat transfer coefficient values vary depending on fluid physical parameters and geometry of heat transfer systems. Such a great number of factors required to be determined causes the necessity to obtain the individual measurements. That mostly involves PCM installations with heat exchangers with complex geometry. In order to measure the heat transfer coefficient during paraffin melting a test facility was set. Its scheme is presented in Figure 1.

A standard refrigerator's condenser was employed in the research (1). It is constructed with a spirally arranged steel coils and fins with round intersection transversely welded. This kind of heat exchanger can be used with PCM tank due to the high density of the fins and properly chosen geometrical parameters of the exchanger.

A 30x15 cm element was cut out of the condenser and placed in the Perspex vessel that was prepared specially for this purpose. Isolation features of this material limit the heat losses to the ambient air. On the other hand its transparency permits the observation of the phase change process directly. The vessel with the investigated element inside was immersed in the paraffin (2). The vessel was installed in a measurement system, as presented in figure 1. The liquid paraffin with an invariable flow was pumped through the exchanger coils. The oil temperature was constant by means of ultrathermostat (4). The temperatures at inflow and outflow to the heat exchanger were controlled continuously during the research. Three thermocouples (3) were applied for that reason. Two of them were located at the liquid paraffin inflow and outflow to the coils while the third one registered the temperature inside the ultrathermostat. All the values were recorded by means of data acquisition station DaqLab (8). The station was connected with the PC computer (9) where the experimental data were saved continuously.

The temperature of the liquid paraffin at the inflow to the heat exchanger was kept as constant. Its stabilization, according to the ultrathermostat producer, was controlled with the precision of  $\approx 0.1$  K.

The liquid paraffin mass flow was assessed by

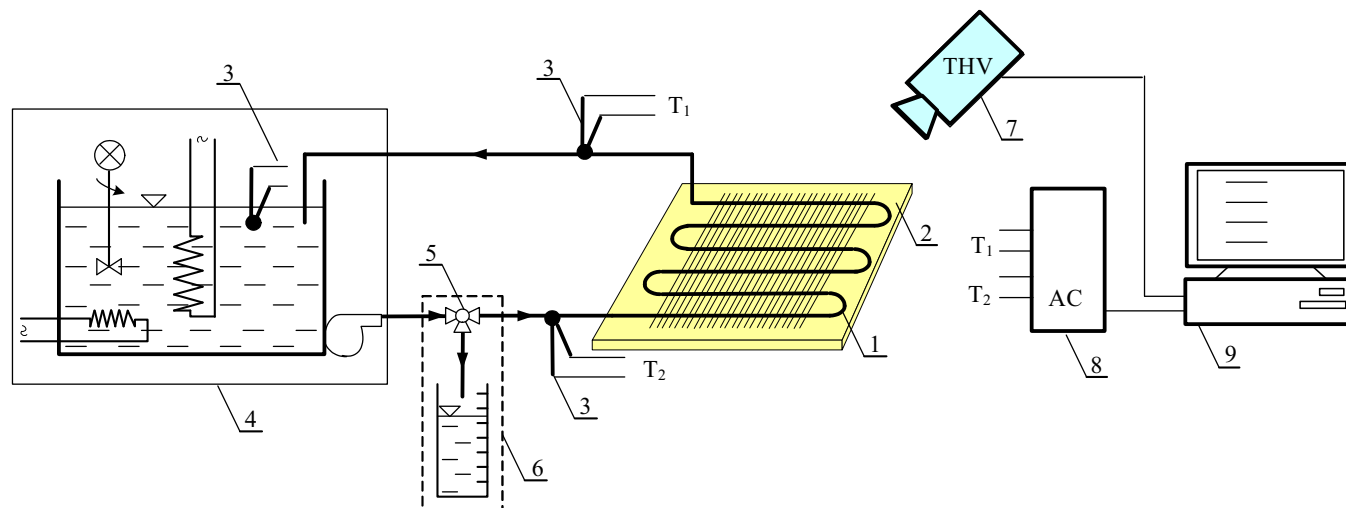


**Figure 1.** Test facility diagram

1-heat exchanger, 2-paraffin, 3-thermocouples, 4-ultrathermostat, 5-three-way valve, 6-mass flow measurement system, 7-infrared camera, 8-data acquisition station, 9-computer

measurement of the fluid volume during the flow through the heat exchanger. In order to conduct the test the liquid paraffin flow to the heat exchanger was interrupted with a three-way valve (5) and the oil volume (6) as well as the filling time were measured. The mass flow was calculated since the dimension of the pipe was known.

The temperature distribution on the outer surface of the condenser was registered by means of infrared camera (7) V50 produced by Polish company Vigo System. The device is equipped with a microbolometric detector with  $384 \times 288$  elements and with the single pixel size of  $25 \times 25 \mu\text{m}$ . Their thermal resolution is lower than 70 mK in 30 °C. The camera operates at a long-wave spectrum of infrared radiation that is 8 – 14  $\mu\text{m}$ . The spatial resolution for a typical lens 35 mm is 0.7 mrad.

Each infrared camera operates according to the individual curve that is extrapolated during the device calibration process against the blackbody. The actual lenses emit not only their own radiation but also the reflected one [23], which influences the final measurement results [24]. The valid temperature reading requires the individual assessment of emission coefficient [25] whose estimation was conducted for the THV camera used in the tests.

The result of the research with the infrared camera is the temperature distribution on the outer surface of the heat exchanger. One of the examples is presented in figure 2. The thermogram shows two adjoining pipes with inflowing hot liquid paraffin. They are joined with

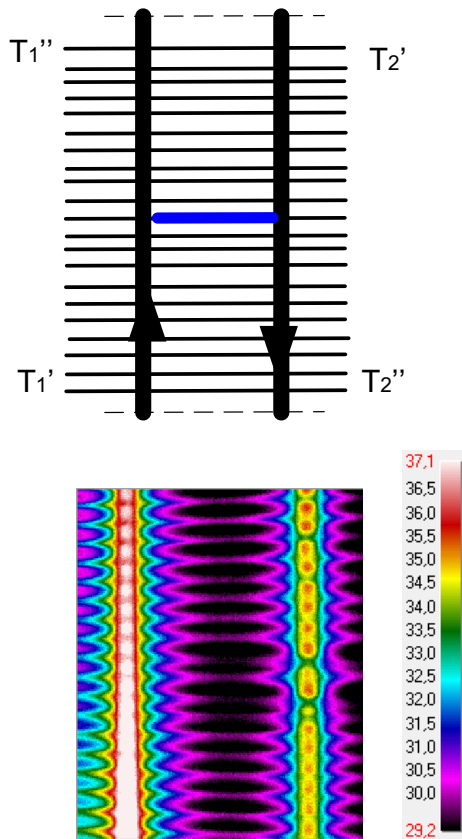


Figure 2. Thermogram of a recurrent element of the condenser.

steel elements in a fin shape, increasing the exchanger surface and intensifying the heat exchange process.

The surface temperature distribution can be read from the presented thermogram. One of the elements was selected as an example and its temperatures were presented in figure 3 where eight curves were shown. Each of them gives the temperatures on the fin every 50 seconds.

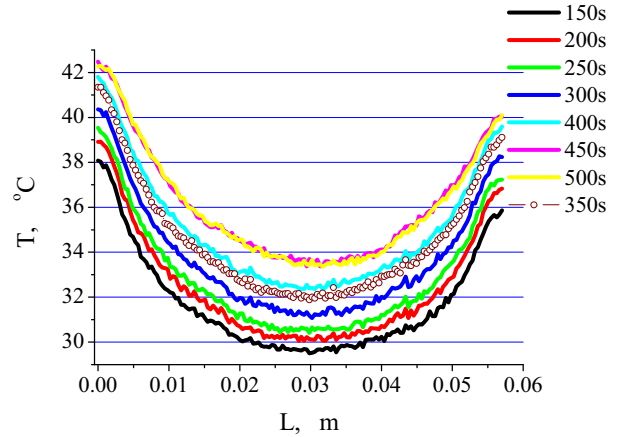


Figure 3. Temperature distribution along the fin

### 3 Results analysis

Heat transfer coefficient is constant in case of free convection and when the temperature change is low. Its value can be assessed by checking the measured temperature field against the analytical fit describing one-dimensional temperature distribution along the fin. In this case the analyzed element was divided in two parts so that the temperature derivative at each end equals zero. It present a fin isolated at one end. For those assumptions, in steady conditions with no internal heat sources, the dependence describing temperature  $T$  distribution along the fin with a fixed cross-section is given [26]:

$$T - T_f = (T_w - T_f) \left( \frac{e^{mx}}{1 + e^{2mL}} + \frac{e^{-mx}}{1 + e^{-2mL}} \right) \quad (1)$$

where:  $T_w$  temperature at the base of the fin, °C,  $T$  current temperature, °C,  $T_f$  ambient temperature, °C,  $L$  fin length, m,  $m$  coefficient for a fin with round intersection, given:

$$m^2 = \frac{\alpha \cdot P}{\lambda \cdot F} \quad (2)$$

where:  $\alpha$  heat transfer coefficient,  $\text{W m}^{-2} \text{K}^{-1}$ ,  $P$  element perimeter, m,  $\lambda$  heat conduction coefficient,  $\text{W m}^{-1} \text{K}^{-1}$ ,  $F$  cross section area,  $\text{m}^2$

The relation (1) can be applied in order to approximate the measured temperature distribution along the fin (see figure 3), which was calculated in each of the time series were conducted. The analyzed element was then considered as a system of two fins connected with the frontal surfaces. The temperatures at the base are different due to the heating process and gradual temperature increase of the liquid paraffin flowing through the heat exchanger. That is why we initially

observe the difficulties in assessing the differences in heat transfer coefficient values for each of the fin. That is why the model (1) fit of the temperature distribution measured was conducted for each of the measurements individually applying the minimum mean square error assumption.

The approximation was performed for 0-1 system. The dimensionless proportion was assumed with the suitable temperature differences. The difference between the temperature on the fin and the minimal temperature for the fin system connected with the frontal surfaces was divided by the difference of temperature at the base of the fin and the minimal one. Next, the heat transfer coefficient was calculated for each of the measurements. An approximation for one of the time series ( $t = 350$  s) is presented in figure 4 as an example. In this case heat transfer coefficient is  $51 \text{ W m}^{-2} \text{ K}^{-1}$  on the left side of an analyzed element and  $48 \text{ W m}^{-2} \text{ K}^{-1}$  on the right one. Similar calculations were performed for all the experimental data receiving approximate heat transfer coefficient values.

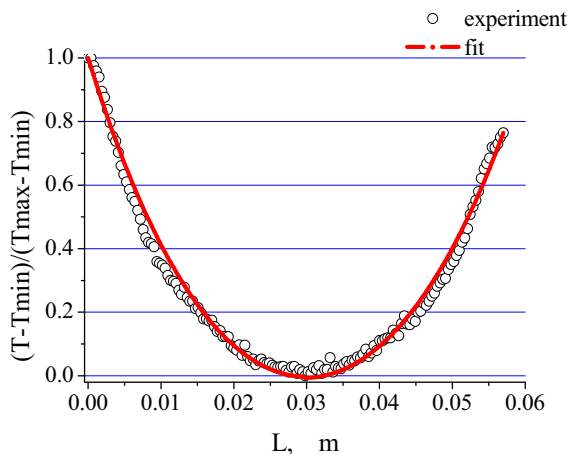


Figure 4. Temperature distribution along the fin for  $t = 350$ s.

The identical procedure was applied for all the results jointly, which is presented in figure 5. Mean heat transfer coefficient value for the investigated condenser on the left and right side of the fin are different from each other and they amount to  $50 \text{ W m}^{-2} \text{ K}^{-1}$  and  $47 \text{ W m}^{-2} \text{ K}^{-1}$ , respectively. As proved, the values do not diverge from analogically calculated values in each of the time series.

The method error was assessed applying the standard deviation value. It was calculated on the basis of the points distance from the approximation curve for the temperature distribution along the fin (see figure 5). The results are shown in figure 6. The calculated value of standard deviation is  $Sd = 0.04 \text{ K}$ . The little value validates the physical similarity of the phenomenon on the considered element, what proves the quasi-stationary process. Therefore the given attempt to impose results in the constant system response with accurate precision. In the analyzed case the temperature increase at the fin base presents an almost parallel displacement of the temperature distribution (see figure 3).

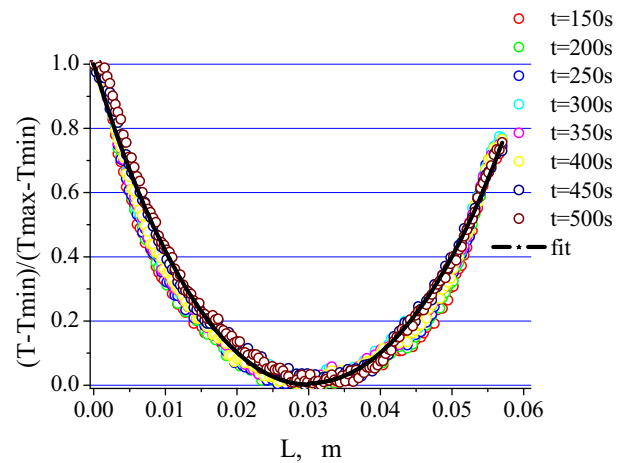


Figure 5. Temperature distribution along the fin for all the experimental data.

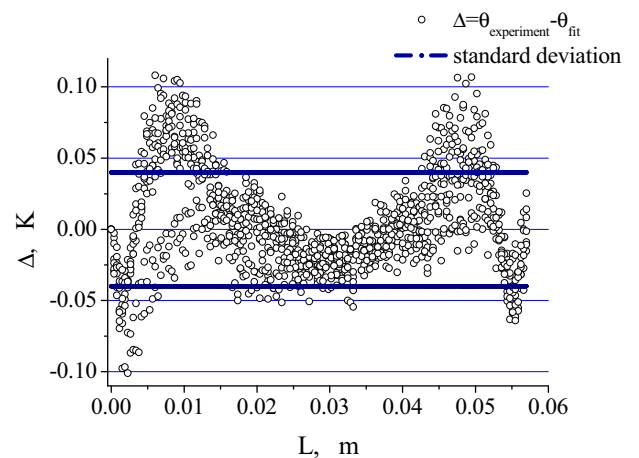


Figure 6. Comparison of measured and approximated temperatures.

## 4 Conclusions

This paper proposes the heat transfer coefficient measurement methodology for the refrigeration's condenser, which is immersed in a vessel with paraffin. Heat source is liquid paraffin that flows through coils in a serpentine shape. The applied heat exchanger is finned with crosswise steel rods in order to improve the heat transfer process. The measurements were conducted for a system presented in figure 1. The temperature field on the outer exchanger surface was examined with an infrared camera with a constant frequency. The temperatures on the fins' surfaces were selected basing on the temperature distribution. The authors' methodology to assess the heat transfer coefficient was developed for an analyzed element. It was discovered that the system is in quasi-stationary state after a period of time, as shown in figure 6.

The result of the calculations is mean heat transfer coefficient for the considered time series. It is equal  $50 \text{ W m}^{-2} \text{ K}^{-1}$  and  $47 \text{ W m}^{-2} \text{ K}^{-1}$  on the left and right side of the fin, respectively. The distance between the experimental data and the curve describing the temperature distribution was assessed with the standard deviation. In this paper its value is low  $Sd = 0.04 \text{ K}$  (see figure 6). It proves the quasi-stationary process thesis and

effectiveness of the chosen methodology for heat transfer coefficient measurement.

## References

1. P. Charvat, J. Stetina, O. Pech, L. Klimes and M. Ostry, EPJ Web of Conferences **67**, 02046 (2014)
2. P. Charvat, O. Pech and J. Hejcik, EPJ Web of Conferences **45**, 01127 (2013)
3. N. Soares, J.J. Costa, A.R. Gaspar, P. Santos, Energ Buildings **59** (2013)
4. M. Pomianowski, P. Heiselberg, Y. Zhang, Energ Buildings **67** (2013)
5. S. E. Kalnæs, B. Pe. Jelle, Energ Buildings **94** (2015)
6. E. Rodriguez-Ubinas, L. Ruiz-Valero, S. Vega, J. Neila, Energ Buildings **50** (2012)
7. X. Shia, Sh. Ali Memon, W. Tang, H. Cui, F. Xinga, Energ Buildings **71** (2014)
8. P. Wang, N. Li, Ch. Zhao, L. Wu, G. Han, Procedia Engineering **71** (2014)
9. A. Tyburczyk, Logistyka, **4** (2015)
10. T. Orzechowski, K. Stokowiec, COW, **44/1** (2013)
11. K. Pielichowska, K. Pielichowski, Progr Mat Sci **65** (2014)
12. Y. Yang, J. Luo, S. Li, G. Song, Y. Liu, G. Tang, Sol Energ Mat Sol C **139** (2015)
13. L. Fan, J.M. Khodadadi, Renew Sust Energ Rev **15** (2011)
14. Z. Yu, G. Cheng, Y. Hu, Energ Convers Manage **80** (2014)
15. B. Xu, Z. Li, Appl Energ **121** (2014)
16. A. R. Archibold, M. M. Rahman, J. Gonzalez-Aguilar, D. Y. Goswami, E. K. Stefanakos, M. Romero, Energy Procedia **57** (2014)
17. N. Şahan, M. Fois, H. Paksoy, Energ Mat Sol C **137** (2015)
18. N. S. Dhaidan, J. M. Khodadadi, Renew Sust Energ Rev **43** (2015)
19. C. Barrenechea, H. Navarro, S. Serrano, L. F. Cabeza, A. I. Fernández, Energy Procedia **57** (2014),
20. R. Pastuszko, Int. J. Therm Sci, **49** (2010)
21. R. Pastuszko, T. M. Wójcik, Exp Therm Fluid Sci, **63** (2015)
22. T. Orzechowski and A. Tyburczyk, EPJ Web of Conferences, **67** (2014)
23. T. Kruczek, Energy, **91** (2015)
24. T. Kruczek, Energy, **62** (2013)
25. M. Pešek and M. Pavelek, EPJ Web of Conferences, **25** (2012)
26. F. P. Incropera, D.P. DeWitt, T.L. Bergman, A.S. Lavine, *Fundamentals of Heat and Mass Transfers* (John Wiley & Sons Inc., U.S.A, 2006)